

Article

A New Approach for Grid-Connected Hybrid Renewable Energy System Sizing Considering Harmonic Contents of Smart Home Appliances

Ayşe Kübra Erenoğlu¹, Alper Çiçek¹, Oktay Arıkan¹ , Ozan Erdinç¹ and João P. S. Catalão^{2,*} 

¹ Department of Electrical Engineering, Yıldız Technical University, 34220 Esenler-Istanbul, Turkey; erenayse@yildiz.edu.tr (A.K.E.); alper_cicek92@hotmail.com (A.C.); oarikan@yildiz.edu.tr (O.A.); oerdinc@yildiz.edu.tr (O.E.)

² INESC TEC and the Faculty of Engineering of the University of Porto, 4200-465 Porto, Portugal

* Correspondence: catalao@fe.up.pt

Received: 25 June 2019; Accepted: 9 September 2019; Published: 19 September 2019



Abstract: Even renewable energy sources provide several advantages, especially from an environmental point of view, where the world has faced great challenges in the last few decades; several negative issues also exist regarding the integration of renewable resources-based power production units in electric power systems. One of the main problems related to pivotal renewable energy resources such as solar, wind, etc., is their stochastic and uncontrollable nature in terms of power production. Therefore, this stochasticity in the supply side of the power system may pose many challenges for system operators. This issue is also problematic for smaller applications where the stochastic production by a main resource, such as a roof-top photovoltaic system, and load demand may not match perfectly at each time instant and therefore should be compensated by additional resources such as battery-based energy storage systems. Herein, the economic considerations to ensure minimum costs for such a hybrid system design are vital so as to increase the penetration of such systems. Therefore, the optimal sizing and planning of hybrid systems have recently gained increasing importance to enhance power system operation in the context of the smart grid paradigm. From a different perspective, harmonics are one of the most important power quality problems in system operations caused by widespread integration of power electronic loads with non-linear characteristics that should be considered. Thus, a new approach for grid-connected hybrid renewable energy system sizing is provided. In order to determine optimal capacities for photovoltaic (PV) and energy storage system (ESS) units for covering residential consumer demand, a mixed integer linear programming (MILP)-based formulation is presented. The main objective is minimizing total costs of the system consisting of investment, capital and maintenance cost functions. A daily power curve is created accurately with real measurements of non-linear loads considering harmonic contents of smart home appliances in Yıldız Technical University, Istanbul, Turkey. In addition, real radiation and temperature values are used in PV production as well as dynamic pricing schemes for realistic evaluations. Moreover, optimal sizing results are compared for both the harmonic-based power curve and rated power curve in terms of satisfying objective function.

Keywords: harmonics; hybrid system; optimal sizing; power quality; smart grid

1. Introduction

1.1. Motivation and Background

In the last few decades, the energy demands of the modern world have extraordinarily increased due to technological innovations, rapid urbanization, and growing population [1]. As a natural

consequence, power-electronic-based electrical equipments have started to be utilized more widely on the demand side [2]. The great achievements of semiconductor technology have captured the electronic industry and dominated the market of household appliances. However, all these paved the way for rising concerns about power quality issues in the distribution system due to the non-linear voltage-current characteristics of these appliances [3]. Therefore, it would not be wrong to mark that utility engineers will encounter harmonic problems more than in the past considering this widespread integration. Several domestic loads such as TV, laptop, printer, computer, light-emitting diodes (LEDs), washing machine, dishwasher, etc., have substantial impacts on the harmonic distortion level in the residential scale [4]. In order to quantify the potential effect on power system operation, the index of total harmonic distortion (THD) is defined as “The ratio of the rms of the high order harmonic components to the rms value of the fundamental quantity, represented as a percentage of the fundamental” [5,6]. According to the Institute of Electrical and Electronics Engineers (IEEE) 519-2014 [7], the voltage THD should be less than or equal to a 5% limit in the point of common coupling measurements from 120 V to 69 kV. Therefore, the harmonic contents of residential loads have to be monitored with digital technology thanks to the smart grid paradigm, and power quality requirements should be controlled in terms of satisfying the standards or not.

From the other perspective, renewable-based energy sources (RESs), such as photovoltaic (PV), have gained increasing interest worldwide and provide great opportunities in terms of covering residential end-users’ power consumption. Integrating these units paves the way for reducing grid dependence, gas emissions, and losses, thus improving the voltage profile and decreasing investment/operation costs [8–10]. Therefore, massive deployment has been performed for every type of end-user thanks to noteworthy attempts from the government and industrial stakeholders. However, the stochastic nature of RESs can cause significant operational problems [11] in the electrical network that should be dealt with. Energy storage systems play an important role considering this issue in terms of aiding to provide a supply–demand balance and also reduce grid dependence. Load fluctuations as well as power variations have been evaluated comprehensively from the power system planner’s perspective and optimal sizing strategies have been proposed in order to provide economical system design. It is important to emphasize that utilizing all the aforementioned benefits strongly depends on how to optimally determine the installation capacities of the system components. Non-optimization based modeling may result in higher investment costs as well as power losses.

1.2. Relevant Literature

A considerable amount of successful studies have been systematically conducted to improve optimal sizing strategies for a hybrid renewable energy system in order to achieve various objectives. The genetic algorithm [12,13], artificial intelligence [14–19], particle swarm optimization (PSO) [20–22], simulated annealing [16], and analytical modelings [23] are commonly used techniques in the literature to solve complex system planning and operation problems.

Among them, Sedighi et al. presented a method for optimal sizing and siting of distributed generation units for the purpose of improving voltage profile and reducing losses as well as THD in distribution networks. Load flows as well as harmonic calculations were taken into consideration in this scheme in which the PSO algorithm was used as a solution technique [20]. Similar to this study [12], the heuristic PSO technique was used in a study by Amanifar and Golshan in [21] to solve optimal distributed generation allocation and sizing problems aiming to minimize investment costs and power losses. A multi-objective distributed generation locating and sizing problem was constructed in a study by Lu et al. in [22] considering the active power loss, harmonic distortion, voltage quality, and voltage sags. Monte Carlo simulation was conducted for fault analysis in order to evaluate the economic losses of the distribution system. Mohanty and Kelapure proposed a methodology for allocating the PV sources in a distribution feeder keeping the voltage THD within permissible limits according to the IEEE-519 standard [24]. Apart from addressing power quality issues, the protection coordination scheme was also taken into account by Rahmani et al. in [12] while providing the optimum distributed

generation sizing. The performance analysis was carried out on an IEEE radial test system and comprehensive evaluations were presented in terms of voltage profile, THD, and power losses.

Combining energy management strategy with optimum hybrid system sizing was presented in a study by Feroldi and Zumoffen in [13] for the purpose of providing loss of power supply probability requirements with the lowest cost. Historical long-term climate and demand data were used in a genetic algorithm-based methodology to testify the impacts of different weather conditions on system design. Hosseinalizadeh et al. developed a techno-economically optimized hybrid system modeling consisting of a wind turbine, PV, a fuel cell, and energy storage system. In this scheme, solar radiation and average wind velocity were considered for investigating different combined RES architectures under diverse sizing scenarios [25].

From the other perspective, an artificial intelligence-based optimization model was presented in a study by Zhou et al. in [14] for both optimum sizing of hybrid PV–wind system and optimum resource allocation based on load demand. It was aimed to decrease high initial and operation costs of the system with proper management strategies and effective modeling techniques. Paliwal et al. presented an approach for an integrated hybrid power system comprising PV–wind–diesel and ESS aimed at determining the optimal mix of mentioned resources by achieving techno-socio-economic criterion. The developed planning formulation was tested under different combined configurations in order to evaluate the reliability needs considering RES uncertainties [15]. For more detailed information about artificial intelligence based-approaches, the studies [16–19] can be also examined.

Askarzadeh developed a novel discrete chaotic harmony search-based simulated annealing algorithm to design an integrated PV–wind–ESS hybrid system optimally in terms of minimizing total annual cost while satisfying the constraints [16]. Escobar et al. proposed an analytical model-based sizing approach for a hybrid PV–wind–hydrogen energy conversion system based on real weather data in order to analyze its feasibility and efficiency [23].

For more information about optimal sizing of hybrid systems, significantly detailed literature surveys on different methodologies, solution techniques, modeling schemes, and discussions are given in [26–32].

The vast majority of studies have also been carried out to investigate the harmonic contents of household appliances and their impacts on system operation. Among them, Neha et al. carried out an experimental analysis for measuring the parameters of THD, displacement power factor (DPF), and transient current of several pieces of equipment by using a multi-function meter in India [33]. Roy and Mather grouped the domestic appliances as lighting, power electronics, resistive, motor, and aggregated loads for establishing a complete bottom-up model to assess voltage stability, harmonics, voltage sag, swells, and unbalance conditions [34]. Also, the load current characteristics were studied in [34]. Harmonic analysis was conducted by Kit et al. in [35] in which the parameters were measured for a desktop computer, fluorescent luminaries, and compact fluorescent lamps and voltage harmonic distortion impacts on current harmonics were also investigated. Grasselli et al. monitored the time-varying harmonic behavior of non-linear residential loads such as a printer, photocopier, cell phone battery charger, and compact fluorescent lamp [36]. Characterization methodology was proposed in [37] for modeling the loads based on their harmonic series composition. Munir et al. in [38], investigated the potential of using PV interface inverters to reduce the effect of harmonics from households. A model for house load and distributed production was created and the model was confirmed by simulations. Egan et al. proposed a model to determine energy consumption with high accuracy for typical Irish dwellings in [39]. However, the effect of harmonic was not taken into consideration in this study. Habib et al. proposed a model to improve the reliability of the power system during a power failure of a shared PV system in [40]. One-year data for the PV system and 10 home consumers for loads were considered. It has been seen that the common use of the PV system makes more profit than the individual use.

These aforementioned references with many other studies not referred here have provided valuable contributions to the literature on the optimal sizing strategies of hybrid systems from different

points of view. Various methods, solution techniques, and modeling frameworks have been presented for achieving different objectives. Nevertheless, it is important to emphasize that most of the reported techniques for optimal sizing of hybrid systems assume sinusoidal operating conditions which do not take the voltage and current harmonics of the demand side into consideration.

1.3. Content, Contributions, and Organization of the Study

In this paper, a mixed integer linear programming (MILP)-based mathematical modeling concept is proposed to find the optimal size of PV and ESS units for covering grid-connected smart home consumption in an economic fashion. The real measurement is performed for residential appliances considering the harmonic components caused by non-linear loads and afterwards the power consumption curve is obtained accurately. The cost function consisting of capital, investment, and maintenance of PV/ESS, is aimed to be minimized after the optimization procedure, thus satisfying the system’s operational constraints. A dynamic pricing scheme is also incorporated into the methodology to determine energy transactions between home and utility grid. To the best knowledge of the Authors, this study attempts to be the first in terms of covering sizing, harmonic impact, dynamic pricing schemes implementation, and real measurements based on gathered data utilization facts in a single study within the existing literature.

The organization of the paper is prepared as follows: Section 2 gives the mathematical background of the proposed optimization problem which is based on MILP with detailed explanations. Section 3 shows the simulation results and the conclusions with possible future studies discussed in Section 4.

2. Methodology

2.1. An Overview of the Presented Structure

The structure of the proposed model is given in Figure 1. In this structure, the smart home has PV and a battery hybrid system. The PV and battery hybrid system both supply energy to the smart home, and even can inject energy to the grid. The smart home can supply energy from the PV system and the battery, and can also buy energy from the grid. The appliances in the smart home consume harmonic loads. In the case of harmonics, more power should be supplied to the load, and this situation changes the system size and operation.

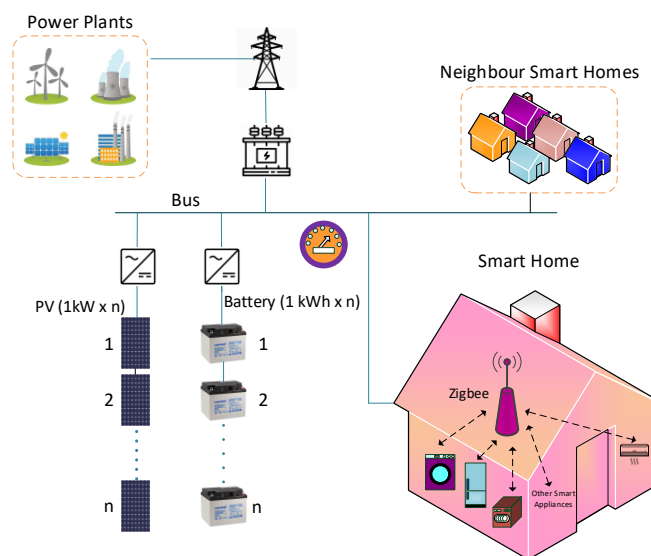


Figure 1. Proposed structure of smart home with photovoltaic (PV)-battery hybrid system.

2.2. Mathematical Formulation

In this study, MILP model of a smart home containing PV and battery hybrid system is presented. It is aimed to maximize the net present value of the profit obtained by a concept containing a PV–battery hybrid system. In addition, economically optimum PV and battery sizes are calculated in this manner. Herein, the profit is acquired by subtracting the expenses from the income with the objective function given below aiming to maximize the net present value of the profit between incomes and the costs.

2.2.1. Economic-Based Formulation

The aim of the problem stated in this study is to maximize total profit and is obtained by subtracting expenses from incomes. The objective function is defined in Equation (1). The aim is to maximize total profit and is obtained by subtracting expenses from incomes.

$$\text{Max. } TNPV = V_{\text{present}}^{\text{income}} - V_{\text{present}}^{\text{outflow}} \tag{1}$$

Equation (2) refers to the balance of power at each time t . Herein, the sum of the power bought from the grid, the power used from the PV, and the power used from the battery is equal to the sum of the power consumed on the loads, the power stored in the battery, and power sold to the grid.

$$P_t^{\text{grid,buy}} + P_t^{\text{PV,used}} + P_t^{\text{bat,used}} = P_t^{\text{load}} + P_t^{\text{bat,ch}} + P_t^{\text{grid,sold}} \tag{2}$$

In Equation (3), the power produced in the PV system is equal to the sum of the power consumed in the system and sold to the grid. n_{PV} refers to the number of 1 kW PV system.

$$P_t^{\text{PV,used}} + P_t^{\text{PV,sold}} = P_t^{\text{PV,prod}} \cdot n_{PV} \tag{3}$$

In addition, Equation (4) expresses that n_{PV} , which is the number of PVs of 1 kW, is less than the maximum number of PVs that is predetermined.

$$n_{PV} \leq n_{PV}^{\text{max}} \tag{4}$$

The power discharged from the battery is either sold to the grid or consumed on loads. This value must also be multiplied by the discharge efficiency. This is described in Equation (5).

$$P_t^{\text{bat,used}} + P_t^{\text{bat,sold}} = P_t^{\text{bat,disch}} \cdot \eta_{\text{bat}}^{\text{disch}} \tag{5}$$

$R_{\text{bat}}^{\text{disch}}$ and $R_{\text{bat}}^{\text{ch}}$ in Equations (6) and (7) indicate the maximum power at which the battery is discharged and charged for a 1 kWh unit, respectively. These expressions are multiplied by n_{bat} to determine the power limits for the battery size.

$$P_t^{\text{bat,disch}} \leq R_{\text{bat}}^{\text{disch}} \cdot n_{\text{bat}} \tag{6}$$

$$P_t^{\text{bat,ch}} \leq R_{\text{bat}}^{\text{ch}} \cdot n_{\text{bat}} \tag{7}$$

As stated in Equation (8), the maximum value is assigned to the number of PV panels with $n_{\text{bat}}^{\text{max}}$ to determine the solution constraints of the optimization problem.

$$n_{\text{bat}} \leq n_{\text{bat}}^{\text{max}} \tag{8}$$

Equation (9) calculates the energy level of the battery at each time t . According to this equation, the energy level at time t is obtained by power at the time $(t - 1)$ with collection by the discharge power

of the battery or by subtracting the charge power in this interval (($t - 1$) to t). Herein, η_{bat}^{ch} is given as the charging efficiency of the battery.

$$E_t^{bat} = E_{(t-1)}^{bat} + P_t^{bat,ch} \cdot \eta_{bat}^{ch} \cdot \Delta T - P_t^{bat,disch} \cdot \Delta T, t > 1 \tag{9}$$

In Equations (10)–(12), the state of energy (SoE) of battery at the initial time, the maximum energy level of battery, and the minimum energy level of battery are defined respectively.

$$E_t^{bat} = E^{bat,ini} \cdot n_{bat}, t = 1 \tag{10}$$

$$E_t^{bat} \leq E^{bat,max} \cdot n_{bat} \tag{11}$$

$$E_t^{bat} \geq E^{bat,min} \cdot n_{bat} \tag{12}$$

Since the battery cannot be charged and discharged at the same time, the u_t^{bat} binary decision variable is defined to prevent this situation. This condition is provided by Equations (13) and (14). Herein, N is defined as a sufficiently big positive number.

$$P_t^{bat,disch} \leq N \cdot u_t^{bat} \tag{13}$$

$$P_t^{bat,ch} \leq N \cdot (1 - u_t^{bat}) \tag{14}$$

The limits of the maximum power that can be withdrawn from the grid and sold to the grid are easily indicated in the Equations (15) and (16), respectively. This is important in terms of grid capacity as the withdrawal of energy from the grid and the sale of energy to the grid cannot be materialized at the same time, therefore u_t^{grid} binary decision variable is defined for this situation.

$$P_t^{grid,buy} \leq P_t^{peak_pwr} \cdot u_t^{grid} \tag{15}$$

$$P_t^{grid,sold} \leq P_t^{peak_pwr} \cdot (1 - u_t^{grid}) \tag{16}$$

The total power injected into the grid is equal to the sum of the power supplied by the PV and the battery. This is described in Equation (17).

$$P_t^{grid,sold} = P_t^{PV,sold} + P_t^{bat,sold} \tag{17}$$

In the case of using PV and battery hybrid system, the change in total electricity cost is explained in Equation (18). $P_t^{grid,buy}$ shows the power bought from the grid. $P_t^{grid,sold}$ represents the power sold to the grid. Furthermore, λ_t^{buy} and λ_t^{sell} are the unit prices for buying and selling, respectively. The prices vary per hour as

$$TCV = \sum_t (P_t^{grid,buy} \cdot \lambda_t^{buy} - P_t^{grid,sold} \cdot \lambda_t^{sell}) \Delta T \tag{18}$$

The calculation of the cost difference between the situations where the PV and battery hybrid system is considered and the neglected is realized in Equation (19).

$$V^{cost_red} = VCB - TCV \tag{19}$$

The total value of cash incomes and outflows during the project lifetime (generally considered as 20 years) is calculated respectively in Equations (20) and (21).

$$V_{present}^{income} = \sum_n \left(\frac{V^{cost_red}}{d_n} \right) \tag{20}$$

$$\begin{aligned}
 &V_{present}^{outcome} \\
 &= C_{cap}^{PV} \cdot n_{PV} + C_{cap}^{bat} \cdot n_{bat} \\
 &+ \sum_n \left(\frac{C_n^{PV,rep,ind} \cdot C_n^{PV,rep} \cdot n_{PV} + C_n^{PV,main} \cdot n_{PV} + C_n^{bat,rep,ind} \cdot C_n^{bat,rep} \cdot n_{bat} + C_n^{bat,main} \cdot n_{bat}}{d_n} \right)
 \end{aligned} \tag{21}$$

2.2.2. Harmonic Model

As was mentioned above, the loads in the smart home caused harmonics and the relevant harmonic model is given below. The instantaneous values for voltage and current are given in Equation (22) and (23), respectively. v_n and i_n are the instantaneous voltage and current of the n . harmonic. Furthermore, w_1 represents the angular frequency for the fundamental component. Lastly, θ_n and δ_n are phase angles of n voltage and current harmonics.

$$v(t) = \sum_{n=1}^{\infty} v_n(t) = \sum_{n=1}^{\infty} \sqrt{2} V_n \sin(n\omega_1 t + \theta_n) \tag{22}$$

$$i(t) = \sum_{n=1}^{\infty} i_n(t) = \sum_{n=1}^{\infty} \sqrt{2} I_n \sin(n\omega_1 t + \delta_n) \tag{23}$$

The instantaneous active power expression is given in Equation (24). Herein, the active power is obtained by multiplying the current and voltage with the same frequency. Similarly, the reactive power expression is also expressed in Equation (25).

$$P = \sum_{n=1}^{\infty} V_n I_n \cos(\theta_n - \delta_n) \tag{24}$$

$$Q = \sum_{n=1}^{\infty} V_n I_n \sin(\theta_n - \delta_n) \tag{25}$$

The effective values of current and voltage are given in Equations (26) and (27), respectively. Herein, the effective value is obtained by taking the square root of the sum of the squares of the fundamental component and other harmonic components.

$$I = \sqrt{\sum_{n=1}^{\infty} I_n^2} \tag{26}$$

$$V = \sqrt{\sum_{n=1}^{\infty} V_n^2} \tag{27}$$

Equations (26) and (27) results in calculating the apparent power by indicating Equation (28).

$$S = V \cdot I^* \tag{28}$$

The apparent power can be obtained from active, reactive, and distortion power types as follows:

$$S^2 = P^2 + Q^2 + D^2 \tag{29}$$

where D distortion power is used to define inactive power for current and voltage at different frequencies.

3. Test and Results

The proposed MILP model is tested in the General Algebraic Modeling System (GAMS) v.24.1.3 with the objective of minimizing total cost. The commercial solver CPLEX v.12 by IBM [41] is used as

a solution technique to provide optimal sizing of PV and ESS units by taking into consideration the harmonic current and voltage contents of smart home appliances.

3.1. Input Data

Almost every piece of equipment found in a typical Turkish household is available in the smart home laboratory at Yildiz Technical University as indicated in Table 1. The rated powers and normal operating conditions have different characteristics that should be considered. Therefore, the household power consumption curve is provided based on real measurement data including harmonics (up to 50th) as shown in Figure 2. It is assumed that the household consists of a four-person family, where one of the parents working has this daily load profile. The 24 h demand power is extended for obtaining 8760 h for making yearly analysis. During this period, the load varies to include summer, winter, and other seasons.

Table 1. Electrical appliances in the smart home.

Appliance	Rated Power (kW)	Appliance	Rated Power (kW)
Refrigerator	0.150	Hair straightener	0.055
Iron	2.4	Oven	2.05
Toaster	0.708	Dishwasher	1.7
Kettle	2	Microwave oven	1.18
Hair dryer	1.536	Printer	0.02
LCD-TV	0.09	Air conditioner	1.14
PC desktop	0.05	Washing machine	1.8
PC monitor	0.03	Vacuum cleaner	1.9
LED Lighting	0.035	Laptop	0.03

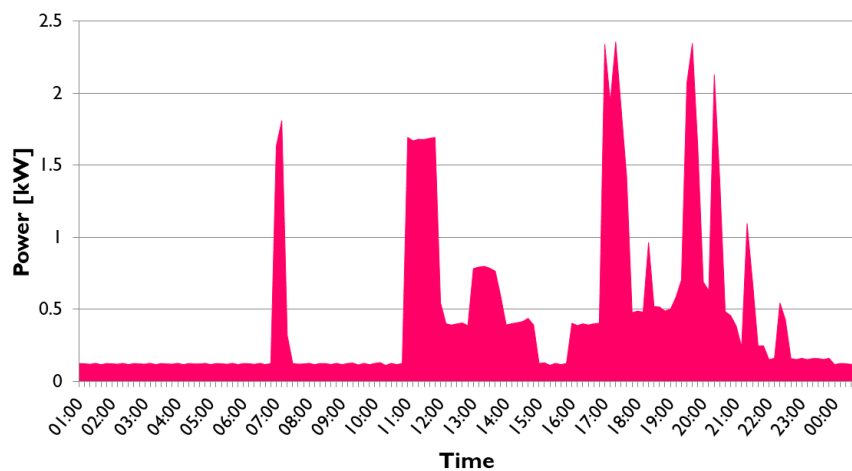


Figure 2. The power consumption of smart home based on real measurements considering harmonic contents.

All appliances are monitored with a professional Fluke Analyzer and the harmonic currents, voltages, THD, and active, reactive and apparent powers are obtained accurately to avoid modeling errors. The Fluke Analyzer can measure and record these values at a desired interval which was selected as three seconds. The power quality measurement of the appliances was experimentally conducted, and real power curve of the smart household was obtained based on the measurements. A representative system establishment for only one appliance can be seen in Figure 3. Some representative appliances are demonstrated with graphs for the sake of clarity for the reader. Figure 4 shows the frequency spectrum of an alternative current (AC) of a washing machine in which the fundamental value is accepted as 100%. It is evidently clear that h_3 and h_5 are most profound components in the working conditions that cause extra power losses similar to PC desktop-oriented measurements depicted in

Figure 5. However, the laptop has different harmonic contents in which h_3 , h_7 , and h_{13} are the dominant values as shown in Figure 6.

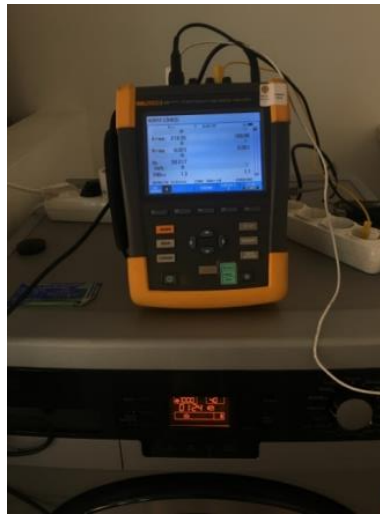


Figure 3. Harmonic measurement of a washing machine.

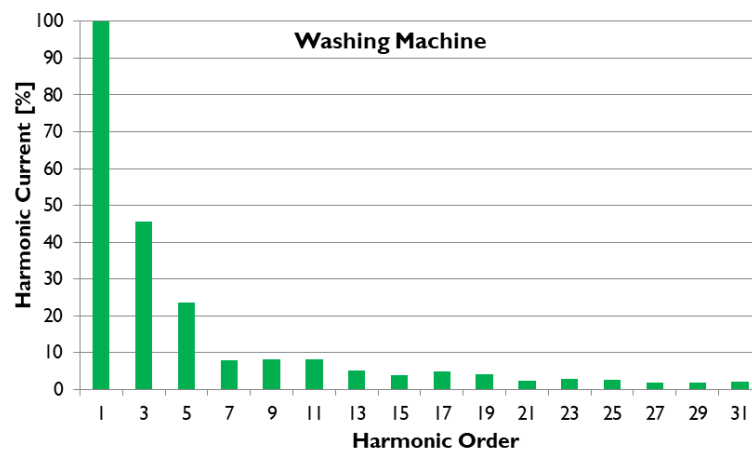


Figure 4. Current spectrum of the washing machine.

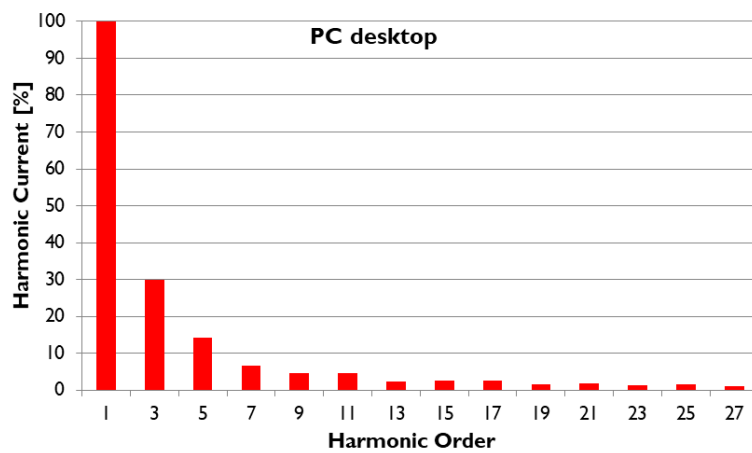


Figure 5. Current spectrum of the PC desktop.

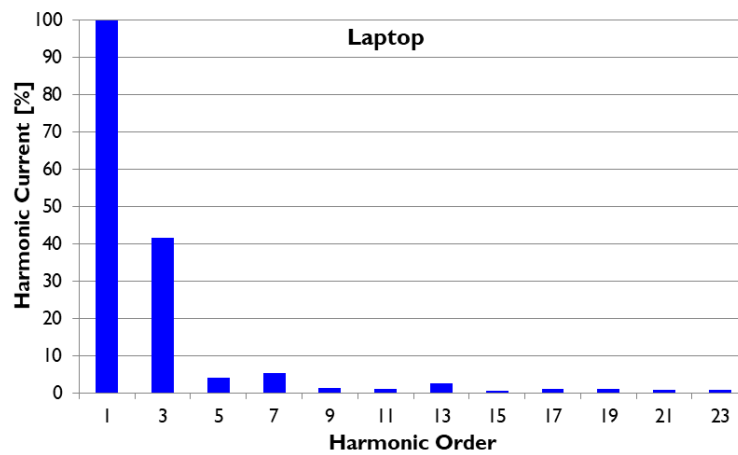


Figure 6. Current spectrum of the laptop.

In order to obtain optimal PV sizing for covering the mentioned demand, real-time measured hourly average power generation data are utilized in the system which was normalized to 1 kW base value in 2013 as shown in Figure 7. Further, 1 kW was accepted as the base power production for PV unit and was multiplied with n_{PV} to find optimal sizing capacity of the system design considering harmonic load, ESS capacity, and grid power transaction under dynamic pricing.

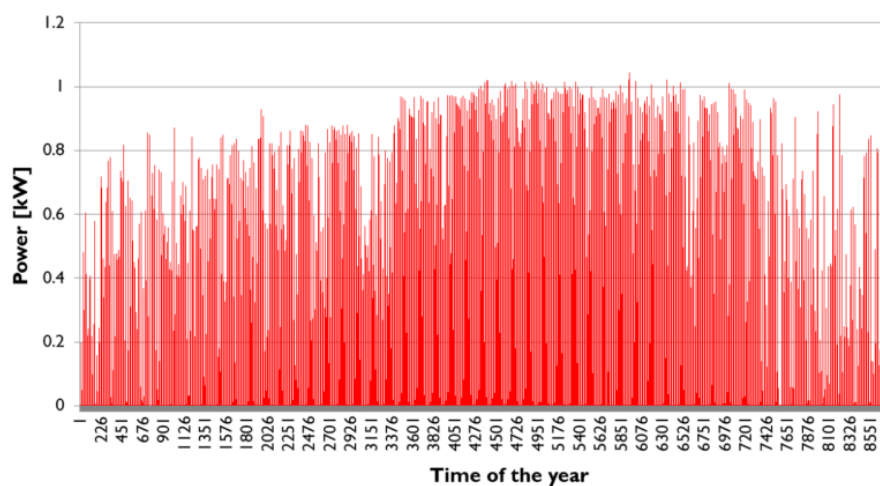


Figure 7. PV system power production as normalized in 1 kW.

On the other hand, it is assumed that the initial SoE of ESS and deep-discharging limit are 0.5 and 0.25 of the relevant maximum battery energy storage capacity, respectively. The charging and discharging efficiencies are also considered as 0.95. When on-site generation is capable of meeting the household demand, the available energy can also be sold to the grid or charge the ESS according to the objective function. A dynamic pricing scheme has an important impact on these axioms due to profit maximization-based optimization model. The buying prices and variation can be seen in Figure 8 based on real-time measurements from the smart meter of a residential end-user [42]. Since the sizing values are determined for a 20-year period, the pricing data is repeated to obtain 8760 h yearly data as similar to the demand curve.

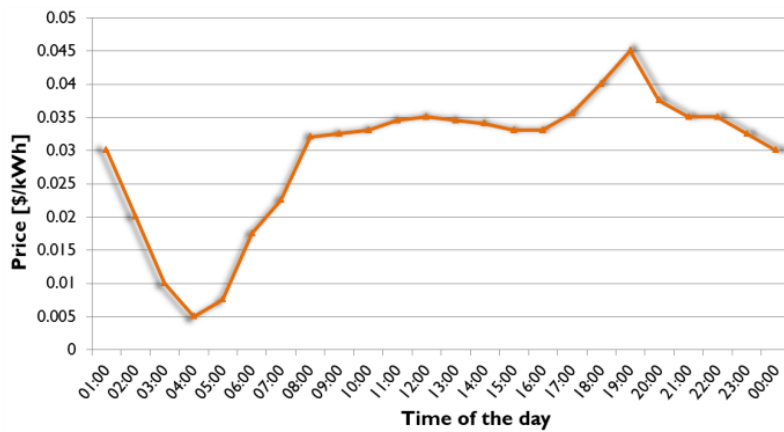


Figure 8. Dynamic pricing of buying energy from a grid.

The input parameters for PV and ESS, as well as economic rates are indicated in Table 2. The costs of capital, replacement, and maintenance can be changed easily when integrating the system for making sensitivity analysis. The optimal sizing results strongly depend on these values. It should be marked that the sizes of PV and ESS are restricted with upper limits of 5 kW and 4 kWh, respectively. However, the flexible scheme enables these inputs to be changed and applies a bigger system for more comprehensive evaluations. Also, the project lifetime is considered as 20 years in which PV is assumed not to need replacement whilst ESS is changed in every 10 years. This is because it is stated by the manufacturers that the PV system has a lifetime of 20 years. For the battery, this value appears to be 10 years in the technical data generally. Therefore, in this study, it was accepted that the lifetime for PV and battery is 20 and 10 years, respectively. However, it is only an input for the proposed structure. The value can be modified as 3, 5, or 7 years if desired in this flexible architecture. What is important in this study is to explain the mathematical background behind the system and show how the decision-making algorithm is working properly.

Table 2. Economic input parameters for PV and ESS units.

Input Parameters	Value
Capital Cost of PV unit (\$/kW)	500
Replacement Cost of PV unit (\$/kW)	500
Maintenance Cost of PV unit (\$/kW]	25
Capital Cost of ESS unit (\$/kWh)	90
Replacement Cost of ESS unit (\$/kWh)	90
Maintenance Cost of ESS unit (\$/kWh)	3
Real Discount Rate	0.05
Project Lifetime (years)	20

Normally, the harmonic currents and voltages are measured in 3 s time granularity, which is convenient to the relevant standards. However, these relatively small intervals would cause a high computation burden while making a plan for 20 years (project time). Therefore, time granularity is selected as an hour for the optimal sizing procedure.

3.2. Simulation Results

In order to investigate the effectiveness of the proposed MILP-based algorithm, two representative results are compared from different points of view. For the sake of a clearer representation, sample cases for Summer and Winter (May 16, 2013 and January 1, 2013) are both analyzed to evaluate operational behavior of optimization strategies.

The power balance of the hybrid system comprising of the power drawn from the grid (buy), the power injected to the grid (sell), battery charging and using values, PV-used power, and electricity demand of end-user are depicted in Figures 9 and 10 for winter and summer days, respectively. At the beginning of the evaluated period, it is seen that the injected power to the grid has increased and reached the maximum value during 01:00 and 02:00 for the winter case. The SoE of the battery is 4 kWh (initial SOE) and it is utilized in selling power as well as covering demand. However, the demand should be provided by only a grid due to low SOE and low buying electricity prices in summer cases as shown in Figure 10.

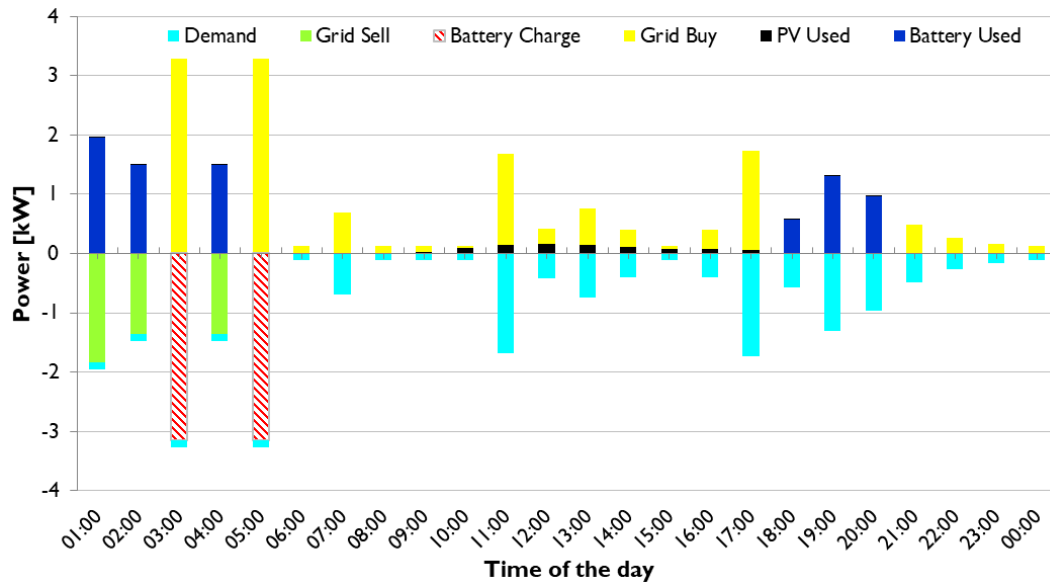


Figure 9. Power balance of the proposed hybrid system for a sample winter case.

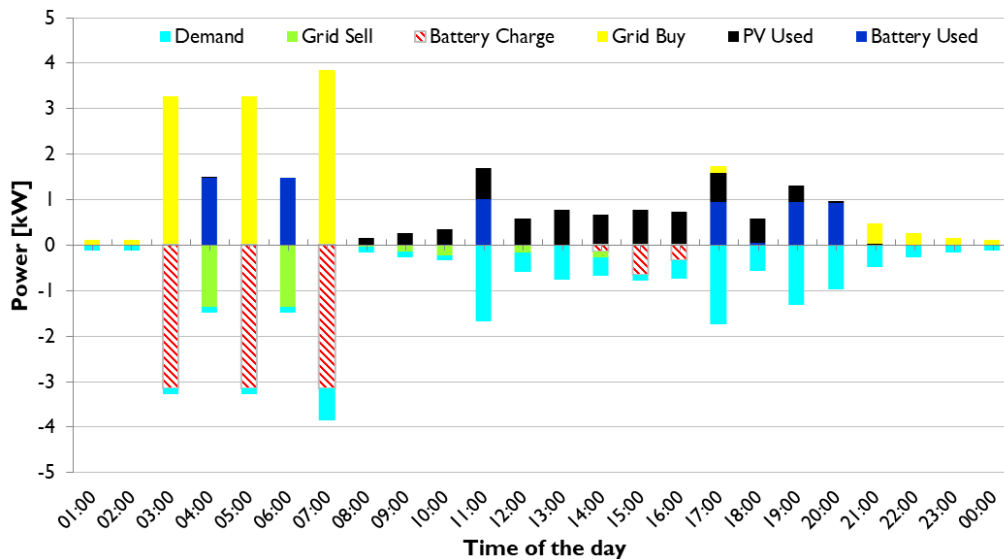


Figure 10. Power balance of the proposed hybrid system for a sample summer case.

At 03:00 and 05:00, the charging power of the battery increases for both case studies due to lower demand and relatively low electricity prices. The power consumption rises at 17:00–20:00, which is to be covered by one of the optimally sized sources for decreasing the total costs. As also seen in Figure 11, the battery presents a good opportunity leading to the possibility of charging at low-priced periods and discharging at peak-demand periods. Therefore, it can be indicated that the existence of a battery in the

hybrid system provides operational flexibility and the charging/discharging periods of this dynamic component are determined by the developed algorithm considering objective function maximization.

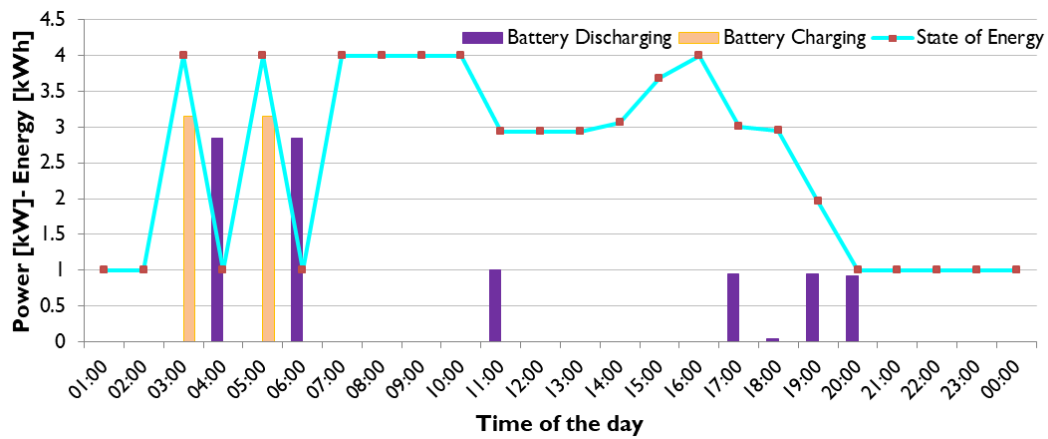


Figure 11. Battery charging and discharging power along with state of energy variation for sample winter case.

The PV power production begins at nearly 08:00, reaches its maximum value (0.16 kW) at 12:00 and finishes at 18:00 for the winter case as illustrated in Figure 12. It is evidently clear that the amount of PV production is not enough for even supplying of the load consumption and as a result injecting power to the grid is zero. On the other hand, the summer case starts earlier than the winter case at 07:00, reaches nearly 0.8 kW value at 14:00 and ends at 21:00 as shown in Figure 13. The battery discharging is utilized to meet the high power consumption at 11:00 without transferring power from the grid due to relatively higher prices. Therefore, the algorithm gives a signal to utilize distributed generation instead of the grid after an economical decision-making process.

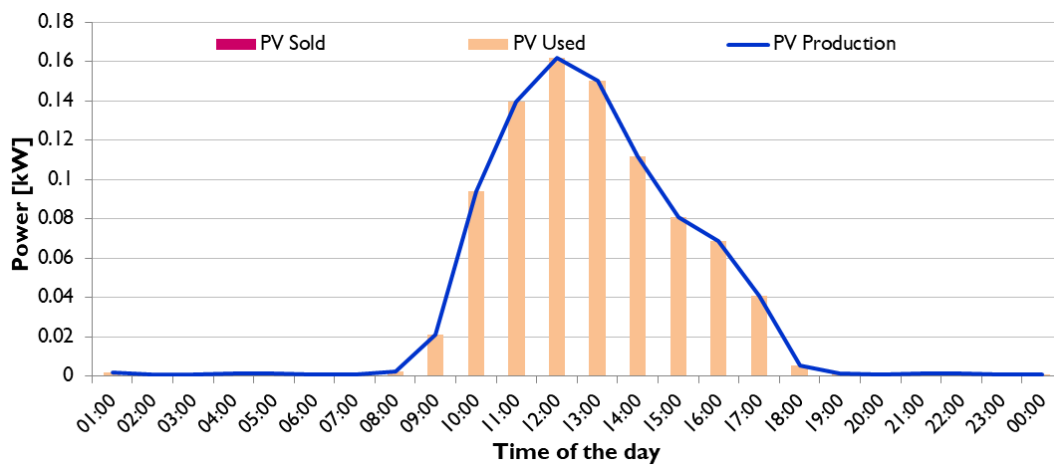


Figure 12. The PV system power decomposition for sample winter case.

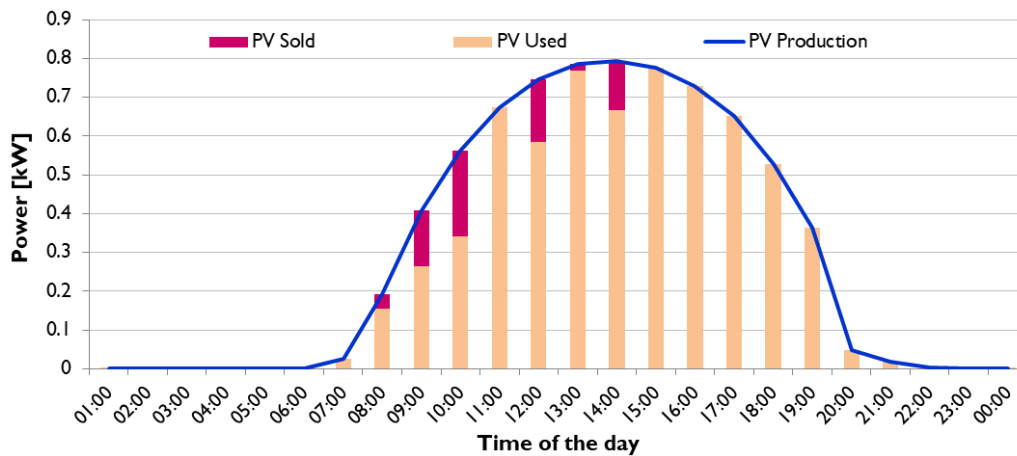


Figure 13. The PV system power decomposition for sample summer case.

During the period from 12:00 to 16:00, even though a certain part of the demanded power can be matched with battery apart from PV, the system decides to use the energy of battery even after 17:00 as the buying prices are becoming higher in peak a period that makes sense to explain this condition. However, it is not right to say the same things for the summer case. Within these periods, high power generation supplies the demand and charges the battery as well as injects available power to the grid.

The ever-increasing power consumption of a smart home especially for 17:00, 19:00, and 20:00 causes discharging power to increase for the purpose of decreasing transferred power from the grid due to high electricity prices. It is strongly encouraged to utilize distributed generation as much as possible instead of utility grid. In the winter case, the charged battery (at 03:00 and 05:00) is discharged and SOE decreases at the depth-of discharge level (1kWh). After 21:00, PV output power becomes zero and battery does not have enough energy to be discharged. Therefore, the demand is covered only by the grid. In order to simplify interpretation of the results for the considered winter and summer, Figures 14 and 15 are depicted to clearly show the decomposition of the injected power.

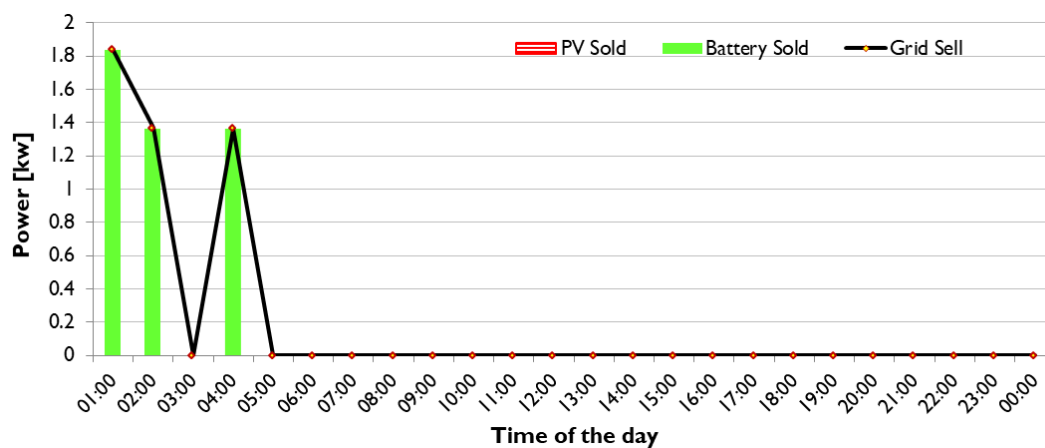


Figure 14. The decomposition of injected power to the grid with PV and battery for sample winter case.

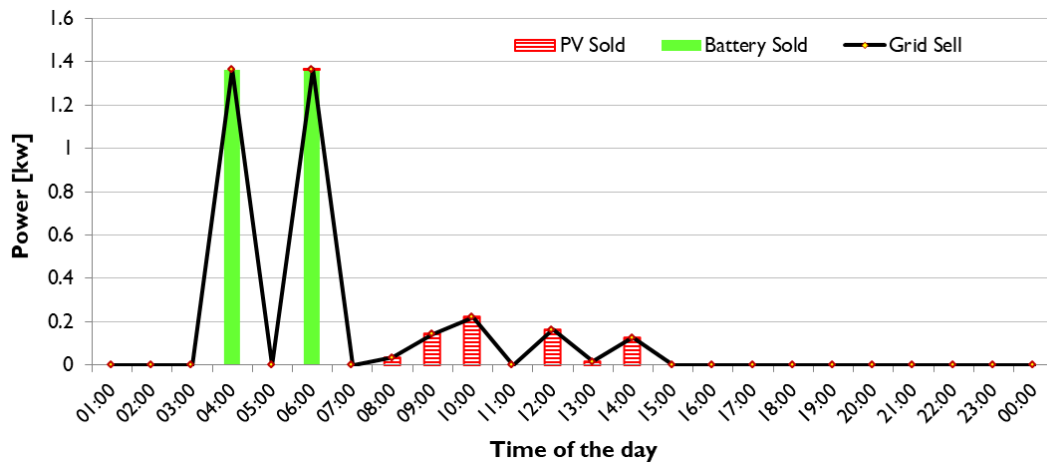


Figure 15. The decomposition of injected power to the grid with PV and battery for sample summer case.

From the economical evaluation perspective, the proposed scheme decides the requirement of 4 kWh battery storage system and 0.81 kW PV unit. After optimal sizing strategy, $V_{present}^{income}$ is obtained as \$1338.379 while $V_{present}^{outcome}$ is \$1171.741. Total profit of the system is \$166.6377 when considering harmonic contents of voltage and current based on real measurements.

In order to investigate harmonic impacts on optimal configuration planning, the power curve of the smart home is created without harmonic components. After simulation results, \$1320.501, \$1155.049, and \$165.4518 is achieved for $V_{present}^{income}$, $V_{present}^{outcome}$, and total profit of the hybrid system, respectively. The relevant results are given in Table 3. On the other hand, 0.79 kW PV and 4 kWh battery storage capacity is obtained after simulation results when harmonics are beyond the scope. As a result, it is not wrong to mark that harmonics do not have great effects on sizing strategies especially for one residential end-user. However, as the number of considered households increase, this impact may be far more obvious. Especially if the developed framework can be applied to industrial and commercial end-users which have densely non-linear loads, the impact of sizing can be significantly obvious. Harmonic loads cause the harmonic currents to be drawn from the grid. For this reason, the actual value of current and voltage are rising which increases injected power from the upstream grid. Increased total load requires increasing the sizing of distributed system components. As a result, PV and battery sizes increase comparing both harmonic-based load case study and non-harmonic-based situation. According to the results, it can be concluded that there is no great impact on cost values for two conditions due to only taking one household into account.

Table 3. Comparison of impacts of harmonic and non-harmonic loads in terms of cost.

Situations	Income Value	Outcome Value	Value of Total Profit of Hybrid System
Without Harmonic	\$1320.501	\$1155.049	\$165.4518
Included Harmonic	\$1338.379	\$1171.741	\$166.6377

4. Conclusions and Discussion

In this study, a MILP model was proposed for sizing a PV and battery hybrid system for a grid connected smart home. Compared to the other existing studies in the area, the harmonic load situation was taken into account in this study and the optimum size of PV and battery was determined for this situation. It should be underlined once again that the study was realized under real power, current, voltage, and harmonics of smart home appliances in Yildiz Technical University, Istanbul, Turkey. Several case studies based on real measurements for the hybrid system and the loads were conducted to assess the impacts of the proposed methodology. The appliance level harmonic components were

considered to have a bottom-up approach for the cumulative impacts of non-linear loads based harmonic components.

The impacts of harmonic were found to be at lower levels for an assessment based on just a single household. However, the increase of the number of households and especially consideration of different end-user types such as commercial and industrial with high levels of non-linear loads will show far more clearly the impacts of harmonic components on sizing purposes. Herein, this study can be a starting point for the relevant literature to consider harmonic components within such studies and the smart home-based residential case can here be assumed just as an example for more dominant industrial and commercial load-based sizing studies.

Therefore, in addition to the proposed work, the consideration of different end-user types, the consideration of harmonic filtering benefit and cost, and the load shifting possibility via an energy management system can be listed as possible future directions of the study both for the Authors of this work and other researchers in the area.

Author Contributions: A.K.E. and A.Ç. mainly contributed by realizing the relevant implementations regarding the formulization and experimental data gathering, and wrote the main parts of the paper. O.A. and O.E. provided the main idea, and coordinated the overall study. J.P.S.C. contributed by overall technical suggestions through the research steps and also contributed to the writing of the final research paper.

Funding: J.P.S. Catalão acknowledges the support by FEDER funds through COMPETE 2020 and by Portuguese funds through FCT, under POCI-01-0145-FEDER-029803 (02/SAICT/2017).

Conflicts of Interest: The authors declare no conflict of interest.

References

- Alkan, B.; Uzun, B.; Erenoğlu, A.; Erdinç, O.; Catalão, J.P.S. Scenario based analysis of an ev parking lot equipped with a roof-top pv unit within distribution systems. In Proceedings of the 2018 International Conference on Smart Energy Systems and Technologies (SEST), Sevilla, Spain, 18 October 2018. [\[CrossRef\]](#)
- Zheng, G.; Xu, Y. Intelligent harmonic instrument for household appliances based on FFT and newton interpolation algorithm. In Proceedings of the 2009 IEEE International Conference on Intelligent Computing and Intelligent Systems, Shanghai, China, 28 December 2009; pp. 812–815. [\[CrossRef\]](#)
- Farrag, M.E.; Haggag, A.; Farooq, H.; Ali, W. Analysis and mitigation of harmonics caused by air conditioners in a distribution system. In Proceedings of the 2017 Nineteenth International Middle East Power Systems Conference (MEPCON), Cairo, Egypt, 19–21 December 2017; pp. 702–707. [\[CrossRef\]](#)
- Rawa, M.J.; Thomas, D.W.; Sumner, M. Experimental measurements and computer simulations of home appliances loads for harmonic studies. In Proceedings of the 2014 UKSim-AMSS 16th International Conference on Computer Modelling and Simulation, Cambridge, UK, 26–28 March 2014; pp. 340–344. [\[CrossRef\]](#)
- De Capua, C.; Romeo, E. A smart THD meter performing an original uncertainty evaluation procedure. *IEEE Trans Instrum. Meas.* **2007**, *56*, 1257–1264. [\[CrossRef\]](#)
- Farooq, H.; Qian, K.; Farrag, M.E.; Allan, M.; Zhou, C. Power quality analysis of distribution systems incorporating high penetration level of EV battery chargers. In Proceedings of the 2011 21st Int. Conf. Electricity Distribution, Frankfurt, Germany, 6–9 June 2011; pp. 1–4.
- IEEE 519 Working Group. IEEE Recommended Practices and Requirements for Harmonic Control in Electrical Power Systems. *IEEE Stand.* **2014**, 519–2014. [\[CrossRef\]](#)
- Hung, D.Q.; Mithulananthan, N. Multiple distributed generator placement in primary Distribution networks for loss reduction. *IEEE Trans. Ind. Electron.* **2013**, *60*, 1700–1708. [\[CrossRef\]](#)
- Aman, M.M.; Jasmon, G.B.; Mokhlis, H.; Bakar, A.H.A. Optimal placement and sizing of a DG based on a new power stability index and line losses. *Int. J. Elect. Power Energy Syst.* **2012**, *43*, 1296–1304. [\[CrossRef\]](#)
- Naderi, E.; Seifi, H.; Sepasian, M.S. A dynamic approach for distribution system planning considering distributed generation. *IEEE Trans. Power Del.* **2012**, *27*, 1313–1322. [\[CrossRef\]](#)
- Erenoğlu, A.K.; Şengör, İ.; Erdinç, O.; Taşçikaraoğlu, A.; Catalão, J.P.S. Economic Operation of a Micro-Grid Considering Demand Side Flexibility and Common ESS Availability. In Proceedings of the 2018 IEEE PES Innovative Smart Grid Technologies Conference Europe (ISGT-Europe), Sarajevo, Bosnia-Herzegovina, 13 December 2018.

12. Rahmani, R.; Niaki, A.A.; Ahmadi, H.; Sadeghi, S.H.H. Optimal Sizing of DGs for Voltage Profile Improvement and Loss Reduction Considering Harmonic Limits and Protection Coordination. In Proceedings of the 26th Iran Conf Electr Eng ICEE 2018, Mashhad, Iran, 8–10 May 2018; pp. 1148–1153. [[CrossRef](#)]
13. Feroldi, D.; Zumoffen, D. Sizing methodology for hybrid systems based on multiple renewable power sources integrated to the energy management strategy. *Int. J. Hydrog. Energy* **2014**, *39*, 8609–8620. [[CrossRef](#)]
14. Zhou, W.; Lou, C.; Li, Z.; Lu, L.; Yang, H. Current status of research on optimum sizing of stand-alone hybrid solar-wind power generation systems. *Appl. Energy* **2010**, *87*, 380–389. [[CrossRef](#)]
15. Paliwal, P.; Patidar, N.P.; Nema, R.K. Determination of reliability constrained optimal resource mix for an autonomous hybrid power system using Particle Swarm Optimization. *Renew. Energy* **2014**, *63*, 194–204. [[CrossRef](#)]
16. Askarzadeh, A. A discrete chaotic harmony search-based simulated annealing algorithm for optimum design of PV/wind hybrid system. *Sol. Energy* **2013**, *97*, 93–101. [[CrossRef](#)]
17. Merei, G.; Berger, C.; Sauer, D.U. Optimization of an off-grid hybrid PV-Wind-Diesel system with different battery technologies using genetic algorithm. *Sol. Energy* **2013**, *97*, 460–473. [[CrossRef](#)]
18. Kumar, R.; Gupta, R.A.; Bansal, A.K. Economic analysis and power management of a stand-alone wind/photovoltaic hybrid energy system using biogeography based optimization algorithm. *Swarm Evol. Comput.* **2013**, *8*, 33–43. [[CrossRef](#)]
19. Arabali, A.; Ghofrani, M.; Etezadi-Amoli, M.; Fadali, M.S.; Baghzouz, Y. GeneticAlgorithm-Based Optimization Approach for Energy Management. *IEEE Trans Power Deliv.* **2013**, *28*, 162–170. [[CrossRef](#)]
20. Sedighi, M.; Igderi, A.; Parastar, A. Siting and sizing of distributed generation in distribution network to improve of several parameters by PSO algorithm. In Proceedings of the 2010 9th Int Power Energy Conf IPEC 2010, Singapore, Singapore, 27–29 October 2010; pp. 1083–1087. [[CrossRef](#)]
21. Amanifar, O.; Golshan, M.E.H. Optimal Profile, generation placement and sizing for loss and THD reduction and voltage and, improvement in distribution systems using particle swarm optimization sensitivity analysis. In Proceedings of the 16th Electrical Power Distribution Conference, Bandar Abbas, Iran, 16 June 2011; Volume 3, pp. 47–53.
22. Lu, H.; Xu, Y.; Yang, J. Study of distributed generation locating and sizing considering power quality. In Proceedings of the 2015 IEEE 2nd Int Futur Energy Electron Conf IFEEC 2015, Taipei, Taiwan, 1–4 November 2015; pp. 1–6. [[CrossRef](#)]
23. Escobar, B.; Hernández, J.; Barbosa, R.; Verde-Gómez, Y. Analytical model as a tool for the sizing of a hydrogen production system based on renewable energy: The Mexican Caribbean as a case of study. *Int. J. Hydrog. Energy* **2013**, *38*, 12562–12569. [[CrossRef](#)]
24. Mohanty, M.; Kelapure, S. Aggregated rooftop PV sizing in distribution feeder considering harmonic distortion limit. In Proceedings of the 2016 Natl Power Syst Conf NPSC 2016, Bhubaneswar, India, 19–21 December 2016; pp. 1–6. [[CrossRef](#)]
25. Hosseinalizadeh, R.; Shakouri, G.H.; Amalnick, M.S.; Taghipour, P. Economic sizing of a hybrid (PV-WT-FC) renewable energy system (HRES) for stand-alone usages by an optimization-simulation model: Case study of Iran. *Renew. Sustain. Energy Rev.* **2016**, *54*, 139–150. [[CrossRef](#)]
26. Anoune, K.; Bouya, M.; Astito, A.; Abdallah, A.B. Sizing methods and optimization techniques for PV-wind based hybrid renewable energy system: A review. *Renew. Sustain. Energy Rev.* **2018**, *93*, 652–673. [[CrossRef](#)]
27. Al Busaidi, A.S.; Kazem, H.A.; Al-Badi, A.H.; Farooq Khan, M. A review of optimum sizing of hybrid PV-Wind renewable energy systems in oman. *Renew. Sustain. Energy Rev.* **2016**, *53*, 185–193. [[CrossRef](#)]
28. Fadaee, M.; Radzi, M.A.M. Multi-objective optimization of a stand-alone hybrid renewable energy system by using evolutionary algorithms: A review. *Renew. Sustain. Energy Rev.* **2012**, *16*, 3364–3369. [[CrossRef](#)]
29. Upadhyay, S.; Sharma, M.P. A review on configurations, control and sizing methodologies of hybrid energy systems. *Renew. Sustain. Energy Rev.* **2014**, *38*, 47–63. [[CrossRef](#)]
30. Chauhan, A.; Saini, R.P. A review on Integrated Renewable Energy System based power generation for stand-alone applications: Configurations, storage options, sizing methodologies and control. *Renew. Sustain. Energy Rev.* **2014**, *38*, 99–120. [[CrossRef](#)]
31. Singh, G.K. Solar power generation by PV (photovoltaic) technology: A review. *Energy* **2013**, *53*, 1–13. [[CrossRef](#)]

32. Khatib, T.; Mohamed, A.; Sopian, K. A review of photovoltaic systems size optimization techniques. *Renew. Sustain. Energy Rev.* **2013**, *22*, 454–465. [[CrossRef](#)]
33. Neha, C.K.; Hegde, M.; Aher, V.; Hegde, V. Effect of home appliances on power quality of conventional grid. In Proceedings of the 2016 Int Conf Circuits, Control Commun Comput I4C 2016, Bangalore, India, 4–6 October 2016; pp. 1–6. [[CrossRef](#)]
34. Roy, J.; Mather, B. Study of voltage-dependent harmonic characteristics of residential appliances. In Proceedings of the 2019 IEEE Texas Power Energy Conf TPEC 2019, College Station, TX, USA, 7–8 February 2019; pp. 1–6. [[CrossRef](#)]
35. Kit, M.Y.; Tse, C.N.; Lau, W.H. A study on the effects of voltage distortion on current harmonics generated by modern smps driven home appliances in smart grid network. In Proceedings of the 9th IET International Conference on Advances in Power System Control, Operation and Management (APSCOM 2012), Hong Kong, China, 30 September 2013; p. 85. [[CrossRef](#)]
36. Grasselli, U.; Lamedica, R.; Prudenzi, A. Time-varying harmonics of single-phase nonlinear appliances. In Proceedings of the 2002 IEEE Power Eng Soc Winter Meet Conf Proc (Cat No02CH37309), New York, NY, USA, 27–31 January 2002; Volume 2, pp. 1066–1071. [[CrossRef](#)]
37. Bonet, A.M.; Ortega, M.A.; Escrivá, G.E.; Bel, C.Á.; Domijan, A. Characterization methodology for in-home loads based on harmonics. In Proceedings of the 1st IEEE-PES/IAS Conf Sustain Altern Energy, SAE 2009—Proc 2009, Valencia, Spain, 28–30 September 2009; pp. 1–6. [[CrossRef](#)]
38. Munir, M.S.; Li, Y.W. Residential Distribution System Harmonic Compensation Using PV Interfacing Inverter. *IEEE Trans. Smart Grid* **2013**, *4*, 816–827. [[CrossRef](#)]
39. Egan, J.; Finn, D.; Soares, P.H.D.; Baumann, V.A.R.; Aghamolaei, R.; Beagon, P.; Neu, O.; Pallonetto, F.; O'Donnell, J. Definition of a useful minimal-set of accurately-specified input data for Building Energy Performance Simulation. *Energy Build.* **2018**, *165*, 172–183. [[CrossRef](#)]
40. Habib, A.H.; Disfani, V.R.; Kleissl, J.; de Callafon, R.A. Optimal Energy Storage Sizing and Residential Load Scheduling to Improve Reliability in Islanded Operation of Distribution Grids. In Proceedings of the 2017 American Control Conference, Seattle, WA, USA, 24 May 2017.
41. CPLEX 12 Solver Description. Available online: <http://www.gams.com/dd/docs/solvers/cplex.pdf> (accessed on 10 June 2019).
42. Tsui, K.M.; Chan, S.C. Demand response optimization for smart home scheduling under real-time pricing. *IEEE Trans. Smart Grid* **2012**, *3*, 1812–1821. [[CrossRef](#)]



© 2019 by the authors. Licensee MDPI, Basel, Switzerland. This article is an open access article distributed under the terms and conditions of the Creative Commons Attribution (CC BY) license (<http://creativecommons.org/licenses/by/4.0/>).